Polygonal billiards and transport: Diffusion and heat conduction

Daniel Alonso,* A. Ruiz, and I. de Vega
Departamento de Física Fundamental y Experimental, Electrónica y Sistemas, Universidad de La Laguna, La Laguna 38203, Tenerife, Spain

(Received 12 September 2002; published 26 December 2002)

A detail study of the diffusive and heat conduction properties of a family of nonchaotic billiards is presented. For dynamical systems with dynamical instability the relation between transport properties and characteristic quantities of the chaotic dynamics naturally emerge. On the contrary, in dynamical systems without chaos (in the sense of exponential separation of nearby trajectories) much less is known. From numerical simulations we compute several quantities related to diffusion, such as the mean square displacement, the behavior of the hydrodynamic modes for long wavelengths, through the properties of the incoherent intermediate scattering function and the velocity autocorrelation function, in connection with the Green-Kubo formula. The analysis of all these quantities indicates that some systems among the family studied have normal diffusion and others anomalous diffusion. The spectral measure associated with the velocity autocorrelation function is also studied. The same analysis reveals that for all the systems treated there is not a well defined super Burnett coefficient. The heat conduction is also explored and found that, naturally, it is valid for the systems that behave diffusively.

DOI: 10.1103/PhysRevE.66.066131 PACS number(s): 05.45.−a, 05.20.−y, 05.60.Cd, 44.10.+i

I. INTRODUCTION

The connections between dynamical and transport properties in dynamical systems are not completely explored. In the past decade the emphasis on the study of chaotic systems has been fruitful and today there exist beautiful relations between chaotic and transport properties such as diffusion, heat and momentum transport. A set of remarkable results establishes the links between diffusion and microscopic dynamical quantities such as the Kolmogorov-Sinai entropy and the Lyapunov exponents. In the case of other transport coefficients it has been also possible to prove their existence starting at a mechanical level [1–7].

In particular, a full Liouvillian characterization of diffusion in specific chaotic models has illuminated the way in which it is possible to connect the above mentioned microscopic quantities with macroscopic ones [10]. Another important result, for a class of hyperbolic systems (transitive Anosov), is the so-called *chaotic hypothesis* to describe nonequilibrium situations [8]. In all these works the degree of stochasticity needed to consistently describe irreversible phenomena and relaxation comes from the exponential instability of the microscopic dynamics. Nonetheless many questions arise, especially in relation to the necessary conditions that a microscopic motion should have in order to observe normal transport at macroscopic scale.

However there is increasing numerical evidence that systems with weaker dynamical stochasticity may exhibit normal transport [9,11,12]. There is also numerical evidence that systems such as a class of triangular billiards may be mixing [13,14]. Therefore it is interesting to investigate in detail a class of dynamical systems for which no dynamical chaos is present and try to seek their transport properties.

For a pure hyperbolic dynamics we have previously studied the so-called Lorentz channel, a simple Lorentz gas model for which there is normal heat transport [15,16]. In fact this system can be considered a prototype for the so-called escape-rate formalism [7,17] and it can be included in a class of chaotic systems for which many analytical results have been obtained.

We study in this work a modified version of the Lorentz channel in which the chain is made up of triangles instead of semicircles. Our systems are in this case polygonal billiards and therefore *no dynamical chaos* (in the sense of exponential separation of nearby trajectories) is present. To study transport in these systems we analyze the diffusion of particles within the billiard looking at the fluctuations of their positions, in particular the mean square displacement. The polygonal billiards studied are ergodic, so mean time averages are equal to ensemble averages. We explicitly compute the mean square displacement, which defines diffusion, and the next order fluctuation, which defines the super Burnett coefficient. If the mean square displacement grows linearly in time the system is expected to be diffusive.

Nonetheless we would like to examine more carefully if the diffusion equation is valid in the systems studied. We numerically compute, following Van Hove [18], the behavior of the hydrodynamic modes and evaluate the Fourier transform of the particle density of the system for long wavelengths (the intermediate incoherent scattering function [25]).

Moreover, the Green-Kubo formula establishes the relation between the diffusion coefficient and the integrated velocity autocorrelation function. In this respect we have analyzed the decay of the velocity autocorrelation function. The correlation functions are intimately related to spectral functions. The correlation functions and spectral functions are just two representations of the same object. The spectral function is a Fourier transformation of the autocorrelation function. Because of this, we have obtained the spectral measure and made a multifractal analysis of it.

*Email address: dalonso@ull.es

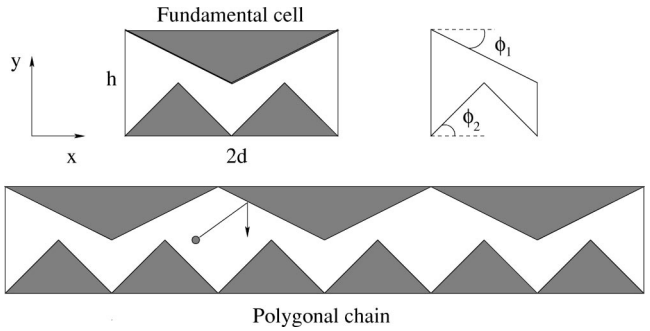

FIG. 1. Schematic representation of the polygonal billiard chain and its parameters. The fundamental cell $\mathcal{D}$ is also shown.

Finally, to enrich the study of transport properties in polygonal billiards we have also investigated the heat conduction in these systems. For this purpose we put our polygonal chain in contact with two heat reservoirs at different temperatures T_0 and T_1. We continue in this way our previous work on heat conduction in the Lorentz channel [16].

The paper is organized as follows. In Sec. II we give a brief introduction of the model we will study. We emphasize the known facts about polygonal billiards that have relevance in our study. In the next section we analyze the diffusion of particles in a polygonal chain. We give a brief theoretical introduction of the quantities we compute. This section is mainly concerned with the mean square displacement as well as the study of the incoherent intermediate scattering function and the dispersion relation for the hydrodynamic modes of diffusion. In Sec. IV we focus on the analysis of the velocity autocorrelation function and spectral measures. In Sec. V we consider the analysis of heat conduction in the polygonal chains studied. Finally in Sec. VI we put together the main conclusions.

II. DYNAMICAL SYSTEM

Since our main interest is to study transport properties and their relation to specific dynamical properties we consider a point particle confined to move inside a periodic chain. The fundamental cell $\mathcal{D}$ of the chain is a polygon in the Euclidean plane $(x,y)=\Re^2$. The border of the cell, $\partial\mathcal{D}$, is composed of straight lines. On the bottom, along the x axis, there is a saw structure with four equal lines forming two identical edges of angle $\pi-2\phi_2$. On the top there are two equal segments forming an edge of angle $\pi-2\phi_1$. The length of the cell along the x axis is $2d$ and h along the y axis. Our billiard is constructed by translations of $\mathcal{D}$ along the x axis. In Fig. 1 we show an schematic representation of the geometry of our system.

If the segments of the polygonal cell form angles that are rationally related to π, then it is said that the polygon is *rational*. On the other hand, if one of the angles is irrationally related to π then it is said that the polygon is *irrational*.

Associated with the billiard table there is a flow $\Phi^t(-\infty<t<\infty)$ in the phase space $\hat{\Gamma}\equiv(x,y,p_x,p_y)$, where (p_x,p_y) is the momentum of the particle. Because of the conservation of energy the motion is confined to a three-dimensional restriction of $\hat{\Gamma}$, i.e., $\Gamma\equiv(x,y,\theta)=D\times S^1$, where θ is the angle of the velocity measured counterclockwise from the positive x axis. The problem scales with energy and therefore we can take the velocity as $|\mathbf{v}|=1$. The flow Φ^t preserves the measure $dx\,dy\,d\theta$. Within the billiard the particle moves freely and suffers elastic collisions at $\partial\mathcal{D}$. The boundary can be parametrized by the arclength s with respect to some origin O. Each collision point is labeled by the impact coordinate s and the projection of the velocity $\mathbf{v}$ with respect to the normal unit vector at the boundary $\mathbf{n}$, i.e., $\mathbf{v}\cdot\mathbf{n}=\cos\theta$. The flow Φ^t induces a mapping ϕ between pairs $(s,\cos\theta)$ that preserves the measure $ds\,d(\cos\theta)$.

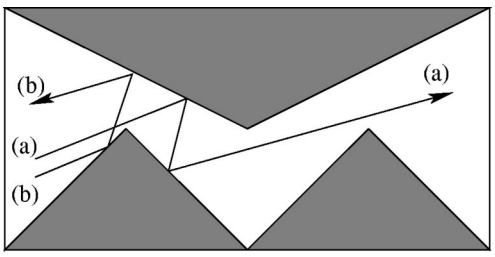

FIG. 2. Typical separation of two initial nearby paths by an edge.

Polygonal billiard tables show a very rich dynamics and are extensively studied in the literature. However, they have attracted much less interest than chaotic billiards. In a polygonal billiard the collisions with the straight segments do not induce chaos. Nonetheless nearby trajectories follow different paths as soon as they meet the vertices of the billiard (see Fig. 2), so some stochasticity may be expected, not from the divergence of nearby trajectories, but from the splitting of the paths at the vertices of the boundary $\partial\mathcal{D}$ [19].

If the billiard is rational the dynamics takes place on a surface S of genus $g(S)\geqslant 1$. S has a nontrivial topology, which is a consequence of the singular character of the vector fields that can be constructed for the dynamics and that are derived from the constants of motion that exist [19]. Such vector fields are singular for a rational polygon and hence S is topologically equivalent to a multihandled sphere. For a simply connected billiard of n rational angles, $\alpha_i=\pi p_i/q_i$ $(i=1,\ldots,n)$, it is possible to give an explicit formula for $g(S)$. Let $\mathcal{N}$ be the least common multiple of q_i, then $g(S)=1+\mathcal{N}/2\Sigma_{i=1}^{n}(p_i-1)/q_i$ [20]. An example of a multiple-connected billiard has been studied in [21]. Trivially, the dynamics is nonglobally ergodic if $g(S)>1$. Nonetheless the flow Φ^t can be decomposed into a one-parameter family of flows Φ_θ^t on the surface S, with $0<\theta<\pi/\mathcal{N}$. The flows Φ_θ^t are called *directional flows* along the direction θ. For almost all angles they are ergodic [20]. It is also known that for a general polygon of n sides there exists a dense set of ergodic polygons. In fact, if a polygon has an irrational angle such that it admits a superexponential fast rational approximation then the dynamics is ergodic. In this sense it is possible to construct irrational polygons that are ergodic [23]. For irrational polygons much less is known, however there are numerical studies, especially for triangles, that give some insight on the properties of the dynamics for irrational polygons. Artuso [13] has shown numerically that they are at

least weakly mixing and the numerical data is not incompatible with mixing. Casati and Prosen [14] extensively studied triangular billiards and their numerical data strongly suggests that irrational triangles are mixing. To date, there is no mathematical theorem that supports these numerical results but, as Gutkin pointed out [22], there is no theorem that precludes the possibility that irrational triangles are in fact mixing.

We present in this work an analysis of the dynamics in a class of irrational polygons. We are particularly concerned with the transport properties that these billiards may develop, such as diffusion, correlation decay, and heat transport.

We have taken our fundamental domain to be an irrational polygon with $\phi_1=(\sqrt{5}-1)\pi/8$ and $\phi_2=\pi/q$ $(q=3,4,5,6,7,8,9)$. We took $h=1$ and $d=h/(\tan\phi_1+\tan\phi_2/2)$; with this choice no particle can travel along the chain without colliding with the boundary of the billiard. Furthermore, the surface available for particles within a fundamental cell is $d/2$, equal for all members of the family of systems. In all our calculations we have used the continuous time as well as the discrete time. But first let us introduce and discuss some relevant concepts for the later developments.

III. DIFFUSION

To study diffusion we start with a system with N (large) particles, such that is possible to define a density $n(x,t)$ that depends on the spatial coordinate x and the time t. This density gives the number of particles located at time t within a small volume dx centered on position x (we suppose a one-dimensional system but generalization to more dimensions is straightforward). Associated with this density we have a mass current $\mathbf{j}(x,t)$. The Fick's law establishes a linear *phenomenological* relation between the small gradient $\nabla n(x,t)$ and the mass current, i.e.,

$$D\nabla n(x,t)=\mathbf{j}, \tag{1}$$

where D is a constant independent of space and time (phenomenological coefficient). Moreover, if there is a local conservation of mass, $\partial_t n+\nabla\cdot\mathbf{j}=0$, then the density $n(x,t)$ satisfies the diffusion equation

$$\partial_t n=D\nabla^2 n \tag{2}$$

and D is the diffusion coefficient. This equation is valid for large systems. If all particles are located at $x=x_0$ at certain initial time $t=0$, then the solution of Eq. (2) is

$$n(x,t)=\frac{1}{(4\pi Dt)^{1/2}}e^{-(x-x_0)^2/4Dt}. \tag{3}$$

One interesting question is related to the specific conditions that a microscopic dynamics should have, such that a large system of particles satisfies a diffusion equation in its time evolution. To be more specific, we can launch an ensemble of particles, construct the spatial distribution $n_a(x,t)$ for different times, and check if the resulting distribution evolves according to Eq. (2).

It is convenient to introduce the Fourier transform $\hat{n}(k,t)$ of $n(x,t)$ as [18,24,25]

$$\hat{n}(k,t)=\int dk\, e^{ikx}n(x,t). \tag{4}$$

If all the particles are initially distributed in the system according to their positions $x_i(t=0)(i=1,\ldots N)$ and because of the time evolution they are at positions $x_i(t)$ at later time t, then the density $n(x,t)$ can be written as the average

$$n(x,t)=\langle\delta(x-[x_i(t)-x_i(0)])\rangle, \tag{5}$$

where the average $\langle\rangle$ is performed over the N particles. The explicit form of the function $\hat{n}(k,t)$ can be obtained combining the last two equations to get

$$\hat{n}(k,t)=\int dk\, e^{ikx}\langle\delta(x-[x_i(t)-x_i(0)])\rangle=\langle e^{ik[x_i(t)-x_i(0)]}\rangle. \tag{6}$$

The function $n(x,t)$ is known, after Van Hove [18], as *self-space-time correlation function* and its Fourier transform $\hat{n}(k,t)$ is called *incoherent intermediate scattering function*. It is obvious that if the self-space-time correlation function satisfies the diffusion equation, with the condition that all particles are located at a single point at the initial time, then the incoherent intermediate scattering function satisfies the diffusion equation in reciprocal space,

$$\partial_t\hat{n}(k,t)=-k^2D\hat{n}(k,t), \tag{7}$$

with the initial condition $\hat{n}(k,0)=1$. This initial value (Cauchy) problem can be solved explicitly to give

$$\hat{n}(k,t)=e^{-k^2Dt}. \tag{8}$$

In this manner the solutions of the diffusion equation are then, with the help of Eq. (4), a linear superposition of *hydrodynamic modes* [40]

$$n_k(x,t)=e^{ikx}e^{-k^2Dt}. \tag{9}$$

These hydrodynamic modes are solutions of the diffusion equation and are spatially periodic with wave number k. They decay exponentially in time, with characteristic time $(Dk^2)^{-1}$. The longer the wavelength of the mode, the larger the decay time. In other words, we have smaller damping, which is a consequence of the mass conservation law [10].

It is convenient for our purposes to introduce, from the incoherent intermediate scattering function, the dispersion relation for the hydrodynamic modes [26]

$$s_k=\lim_{t\to\infty}\frac{1}{t}\ln\hat{n}(k,t)=-k^2D, \tag{10}$$

in terms of which the hydrodynamic modes are expressed as [10]

$$n_k(x,t)=e^{ikx}e^{s_kt}. \tag{11}$$

In general, the diffusion equation is a consequence of a first approximation for the thermodynamic force conjugated to the mass current, which includes only a $\nabla n(x,t)$ term (Fick's law). This leads to a $\nabla^2 n$ term in the diffusion equation. If $n(x,t)$ varies rapidly in space the diffusion equation can be extended to include higher spatial derivatives of $n(x,t)$, such as $\nabla^4 n$. Therefore an extra term, $B\nabla^4 n$, appears in the diffusion equation. B is called the super Burnett coefficient and all that has been said remains valid if B is well defined. If so, a more general expression for s_k follows:

$$s_k = \lim_{t\to\infty} \frac{1}{t} \ln \hat{n}(k,t) = -Dk^2 + Bk^4 + \vartheta(k^6). \tag{12}$$

An interesting feature of the incoherent intermediate scattering function is its relations to the spatial fluctuations. Such relations can be derived in the following manner. First let us notice that $\hat{n}(k=0,t)=1$. The derivatives of $\hat{n}(k,t)$ with respect to k at $k=0$ can be computed; in particular the first derivative is

$$\partial_k \hat{n}(k,t)|_{k=0} = \partial_k \langle e^{ik[x(t)-x(0)]}\rangle|_{k=0} = \langle i\Delta x e^{ik\Delta x}\rangle|_{k=0} = i\langle \Delta x\rangle, \tag{13}$$

where $\Delta x = x(t) - x(0)$. Therefore, the first derivative of the incoherent intermediate scattering function at $k=0$ gives the average value of the fluctuation $x(t)-x(0)$. A similar reasoning leads to an explicit relation between higher derivatives and higher order fluctuations. In particular, the second derivative and the mean square displacement are related as

$$\partial_{kk}^2 \hat{n}(k,t)|_{k=0} = -\langle (\Delta x)^2\rangle. \tag{14}$$

If the diffusion equation holds then the Einstein relation for diffusion follows

$$\langle (\Delta x)^2\rangle = 2Dt. \tag{15}$$

In the same manner it is possible to derive relations involving higher order fluctuations. A short calculation gives the explicit formula

$$\langle (\Delta x)^4\rangle - 3\langle (\Delta x)^2\rangle^2 = 24Bt, \tag{16}$$

which is an Einstein relation for the super Burnett coefficient.

If we center our attention on the mean square fluctuation, it follows that the analytic behavior of the incoherent intermediate scattering function, at least up to order k^2, is required in order for the mean square displacement (15) to be well defined. Indeed if the analytic behavior is satisfied and the Einstein relation (15) holds, then $n(x,t)$ satisfies the diffusion equation.

If the Einstein relation is satified then we speak of *normal diffusion*; on the contrary, we have *anomalous diffusion* if the mean square displacement does not grow linearly in time.

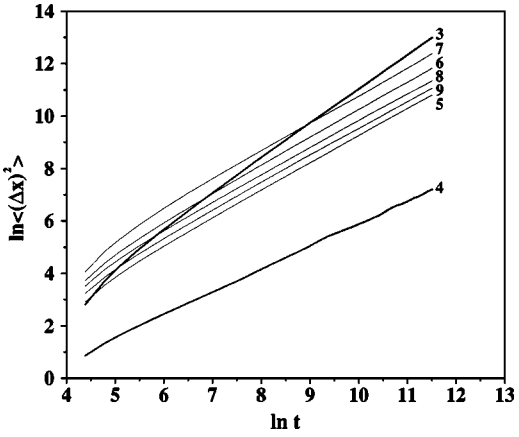

FIG. 3. Mean square displacement of position for $\phi_2 = \pi/q$ ($q = 3,4,5,6,7,8,9$). The label on the right-hand side of each curve indicates the value of q. The simulations were done for 1.2×10^5 particles and up to time $t_f = 10^5$. The value of the slope for each curve is indicated in Table I.

A. Ensemble numerical simulations

In this section we present the results of our numerical simulations concerning the diffusive behavior of the polygonal chain. First we compute the mean square displacement and study its time variation in order to explore the validity of the Einstein relation for diffusion. Due to the geometry of our system the particles have transport along the x direction.

We integrated the motion for 1.2×10^5 particles up to $t_f = 10^5$ continuous time units. The mean square displacement was computed from a Monte Carlo average over the particles. We focused on the cases $\phi_2 = \pi/q$, $q = 3,4,5,6,7,8,9$. Up to the maximum time we have considered the mean square displacement for the $\phi_2 = \pi/3$ system grows as $\sim t^{1.3}$, which reflects a superdiffusive behavior. The case $\phi_2 = \pi/4$ behaves subdiffusively, with $\langle (\Delta x)^2\rangle \sim t^{0.86}$. All the other systems have a power very close to one; from this data we can infer that they satisfy the Einstein relation for diffusion. These results are shown in Fig. 3 and Table I.

The numerical results indicate that the family of systems considered presents both types of diffusive behavior, strange and normal, at least up to the time we can reach in our simulations. As we have previously discussed, we would like to check further the nature of the dynamics of an ensemble of particles within the chain. Another quantity of interest suit-

TABLE I. Diffusion with 1.2×10^5 particles up to a continuous time 10^5. B was obtained from the fitting $\langle (\Delta x)^2\rangle = At^B$.

ϕ_2	B
$\pi/3$	1.30
$\pi/4$	0.86
$\pi/5$	1.03
$\pi/6$	1.04
$\pi/7$	1.06
$\pi/8$	1.01
$\pi/9$	1.01

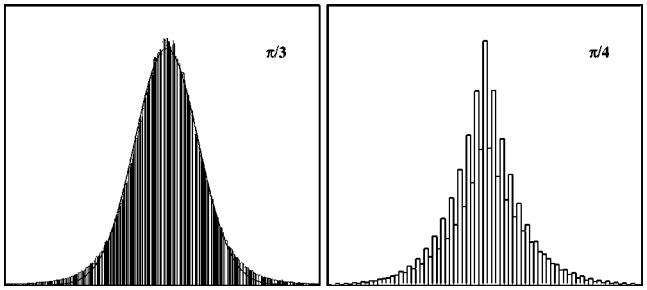

FIG. 4. Histograms of x coordinates for an ensemble of 1.2×10^6 particles at time $t_f=5\times10^3$, for $\phi_2=\pi/3$ and for $\phi_2=\pi/4$. The thick line ($\pi/3$) is the best Gaussian fitting to the data.

able for this purpose is s_k, as defined in Eq. (10), where k is the x component of the wave vector. We limit ourselves to wave vectors along x direction. If the motion is diffusive we should observe that for small values of k the results are compatible with Eq. (10).

To clarify this question the following simulation was done. We took an ensemble of 1.2×10^6 particles and integrated their trajectories up to a time $t_f=5\times10^3$. From the data obtained we constructed the histograms of x positions, which are a numerical approximation of $n(x,t_f)$. In Fig. 4 we show the results for the systems $\pi/3$ and $\pi/4$, and in Fig. 5 the data for the systems $\pi/5$ and $\pi/6$.

The figures also include the best Gaussian fitting (for comparison) of the data. Clearly the $\pi/4$ system is far from a Gaussian shape, meanwhile the other systems seem closer. The tails of the histograms are very well reproduced by a Gaussian profile for $\phi_2=\pi/5$ and $\pi/6$, while the tail of the histogram for the $\phi_2=\pi/3$ system shows some deviations from the Gaussian bell.

We have computed $\hat{n}(k,t)$ from a series of numerical simulations with an increasing number of particles and a fixed value of $k_x=k=0.01, k_y=0$. In all cases it is observed (see Figs. 6, 7, and 8) that the decay in time of s_k is better reproduced when the simulations involve a larger number of particles. The question is if such decay is exponential. In Fig. 9 we have computed $\ln|\ln(\hat{n}(k,t))|$. From the data it seems that the decay is not exponential for $\phi_2=\pi/3$ and $\pi/4$, while for the other cases it seems to be exponential, at least up to the time we are able to reach in our simulations. The data is compatible with $\hat{n}(k,t)=Ae^{-\alpha k^2 t^\beta}$, with $\beta=1$ only for $\phi_2=\pi/q, q=5,6,7,8,9$. In these cases the numerical simulations strongly suggest that the systems behave diffusively and probably develop hydrodynamic modes.

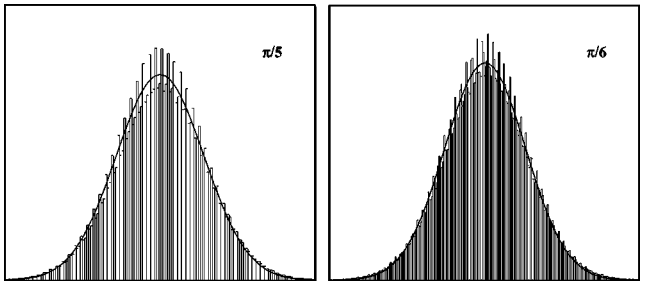

FIG. 5. The same as Fig. 4 for the systems $\phi_2=\pi/5$ and $\phi_2=\pi/6$.

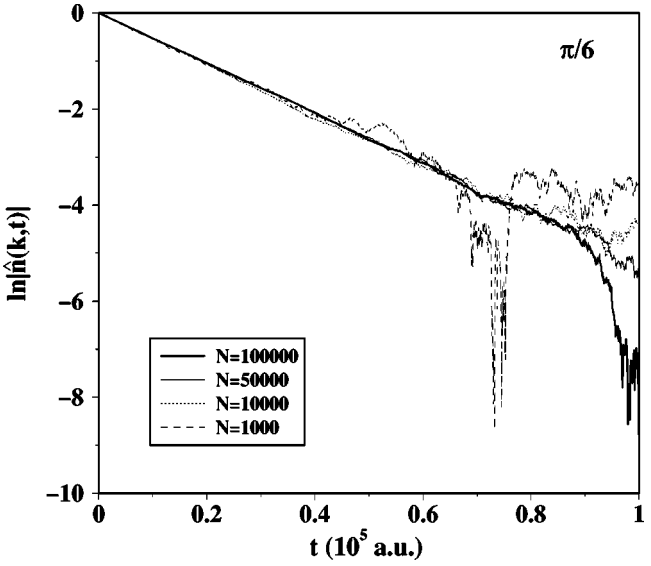

FIG. 6. $\ln|\hat{n}(k,t)|$ vs time for $\phi_2=\pi/6$ computed with an increasing number of particles N. Notice how taking a larger N improves the resolution of the exponential decay. In this figure and in the rest of the paper, a.u. refers to arbitrary units.

We could ask ourselves about the super Burnett coefficient. Our data clearly indicates that the Einstein relation for the super Burnett coefficient is not valid, but we will treat this point in the next section.

B. $\phi_2=\pi/6$ system: single particle simulations

In order to study in more detail a system that shows diffusive behavior, we consider in this section the particular system $\phi_2=\pi/6$. In this case we compute the averages using the long time series generated from a single particle simulation. Throughout the section time is discrete and corresponds

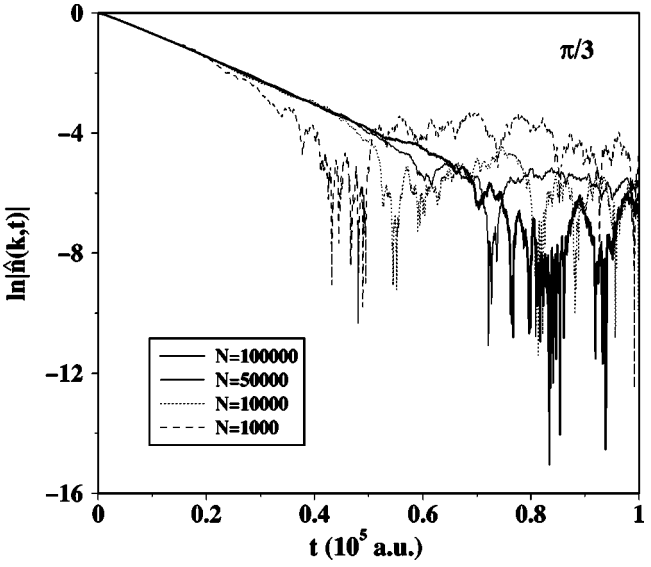

FIG. 7. The same as Fig. 6 for $\phi_2=\pi/3$.

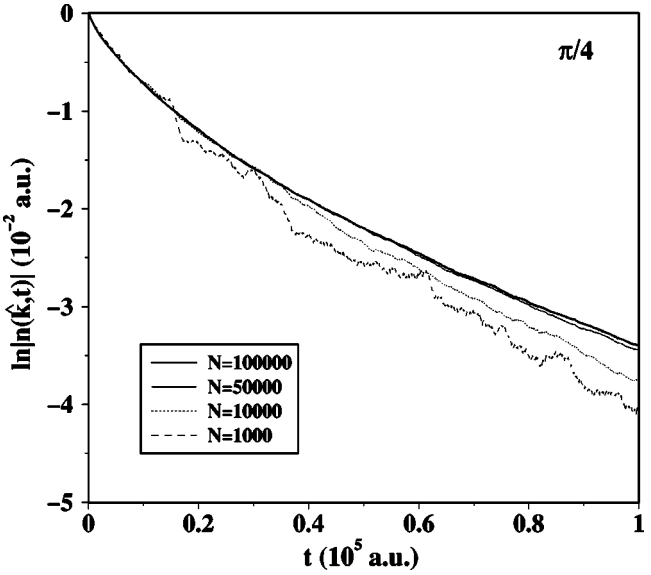

FIG. 8. The same as Fig. 6 for $\phi_2=\pi/4$.

to the collision time. To determine the consequences that the length of the time series has on the numerical results we have used several time series with increasing length.

First we consider the mean square displacement. The results are shown in Fig. 10 for different lengths of the time series. In all the cases a diffusive behavior is clear. The power that gives the growth of the mean square displacement in time is almost one, hence the Einstein relation for diffusion (15) is satisfied.

It is interesting to compute higher order fluctuations. To this aim we have calculated $\langle(\Delta x)^4\rangle$. This average grows quadratically in time as $\alpha_1 t^2+\beta_1 t+\gamma_1$. In the same vein, as $\langle(\Delta x)^2\rangle$ satisfies the Einstein relation (15), the average $3\langle(\Delta x)^2\rangle^2$ also has a quadratic behavior with time, which can be expressed as $\alpha_2 t^2+\beta_2 t+\gamma_2$. Therefore, if there is a well defined Einstein relation for the super Burnett coefficient [see Eq. (16)], it should happen that $\alpha_1=\alpha_2$, in such a way that the difference $\langle(\Delta x)^4\rangle-3\langle(\Delta x)^2\rangle^2$ should grow linearly in time.

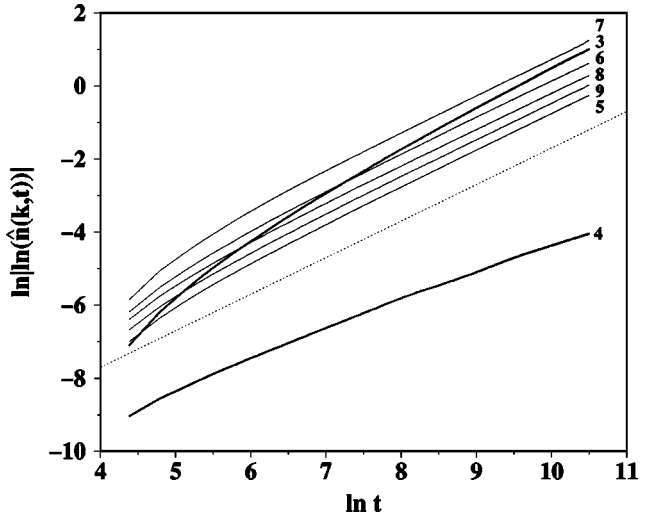

FIG. 9. $\ln|\ln(\hat{n}(k,t))|$ vs $\ln t$ for $\phi_2=\pi/q(q=3,4,5,6,7,8,9)$. The label on the right-hand side of each curve indicates the value of q. The dotted line has slope=1.

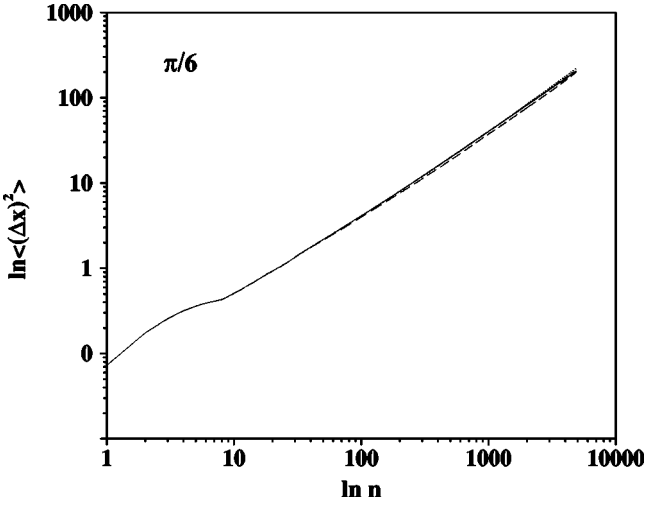

FIG. 10. Mean square displacement computed from a single trajectory with 1.4,7,30, and 49×10^6 collisions in a system with $\phi_2=\pi/6$. As soon as the statistics is improved it is difficult to distinguish the different curves.

Our numerical simulations give clear evidence that for our billiards the Einstein relation for the super Burnett coefficient is ill defined. We have numerically computed the curves for $\langle(\Delta x)^4\rangle$ and $3\langle(\Delta x)^2\rangle^2$ for time series of different lengths. For each curve we fitted the data to a function $\alpha t^2+\beta t+\gamma$ and extracted the coefficients α_1 and α_2. For having a case to compare with, we have done the same evaluations for a Lorentz channel [16]. For this system it is clear that the coefficients α_1 and α_2 get closer as soon as the statistics is improved (see Tables II and III and Figs. 11, 12, and 13). For the polygonal chain the results are drastically different and drive us to the conclusion that there is not a well defined super Burnett coefficient for these systems. So we conclude from these results that the polygonal chain has a well defined Einstein relation for diffusion, but not for the super Burnett coefficient. These results were also observed in our ensemble simulations. The fact that the higher moments of Δx are not defined in a polygonal billiard has been previ-

TABLE II. Coefficients α_1 and α_2 for $3\langle(\Delta x)^2\rangle^2(t)=\alpha_1 t^2+\beta_1 t+\gamma_1$ and $\langle(\Delta x)^4\rangle(t)=\alpha_2 t^2+\beta_2 t+\gamma_2$ in the Lorentz channel. N indicates the length of the trajectory over which averages are evaluated.

$N\times10^5$	α_1	α_2
7	0.06497	0.05737
14	0.05367	0.05103
35	0.05897	0.05796
70	0.05645	0.05260
140	0.06003	0.05914
300	0.06017	0.05955
350	0.06181	0.06152
490	0.06120	0.06125

TABLE III. The same as Table II for the pseudointegrable channel ($\phi_2=\pi/6$).

$N\times10^5$	α_1	α_2
7	0.003719	0.003822
14	0.004916	0.004591
35	0.005576	0.005315
70	0.005077	0.006768
140	0.004912	0.006875
300	0.00523	0.00675
350	0.00504	0.007102
490	0.005088	0.006907

ously studied by Dettmann and Cohen [11]. Let us point out that the disorder of the scatterers plays a role in their results, while in our case the scatterers are ordered.

IV. CORRELATION FUNCTIONS

The nature of fluctuations contained in correlation functions plays a central role in the understanding of transport properties. From the behavior of some autocorrelation functions we can infer if the system will show some transport property. In particular, because of the Green-Kubo formula

$$D=\int_0^\infty \langle v_t v_0\rangle dt, \tag{17}$$

where the average is taken with respect to the proper invariant measure, the decay of the velocity autocorrelation function is crucial to have a well defined diffusion coefficient (for a nice presentation of this subject we refer to [24]).

For this relation to hold, the velocity autocorrelation function should decay fast enough. Therefore it is interesting to analyze in more detail the properties of the correlation functions in our system. With respect to transport, systems with real continuous spectrum and fast enough decay of correlation functions may present Gaussian fluctuations in their approach to equilibrium, in the sense of the central limit theorem. For such systems it is possible to have a well defined transport coefficient. To study this question more deeply let us briefly introduce some concepts which will be useful in the forthcoming discussion.

Let us consider a dynamical system (Φ^t,Γ,μ), where Φ^t is a flow (t maybe discrete) acting on a phase space Γ with an invariant measure μ [33]. A dynamical system is said to be *mixing* if for any pair of functions f and g that belong to the Hilbert space $\mathcal{H}$ of square integrable functions $\mathcal{L}^2(\Gamma,\mu)$ correlation functions decay in time, i.e.,

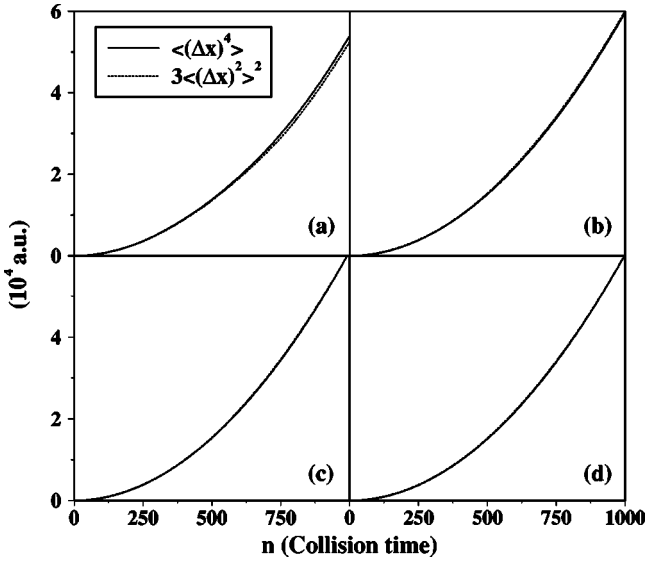

FIG. 12. Comparison of the fluctuation $\langle(\Delta x)^4\rangle$ with $3\langle(\Delta x)^2\rangle^2$ for a single particle simulation for the Lorentz channel. (a) is for a time series up to 7×10^5 collisions, (b) 7×10^6, (c) 1.4×10^7, and (d) up to 4.9×10^7 collisions.

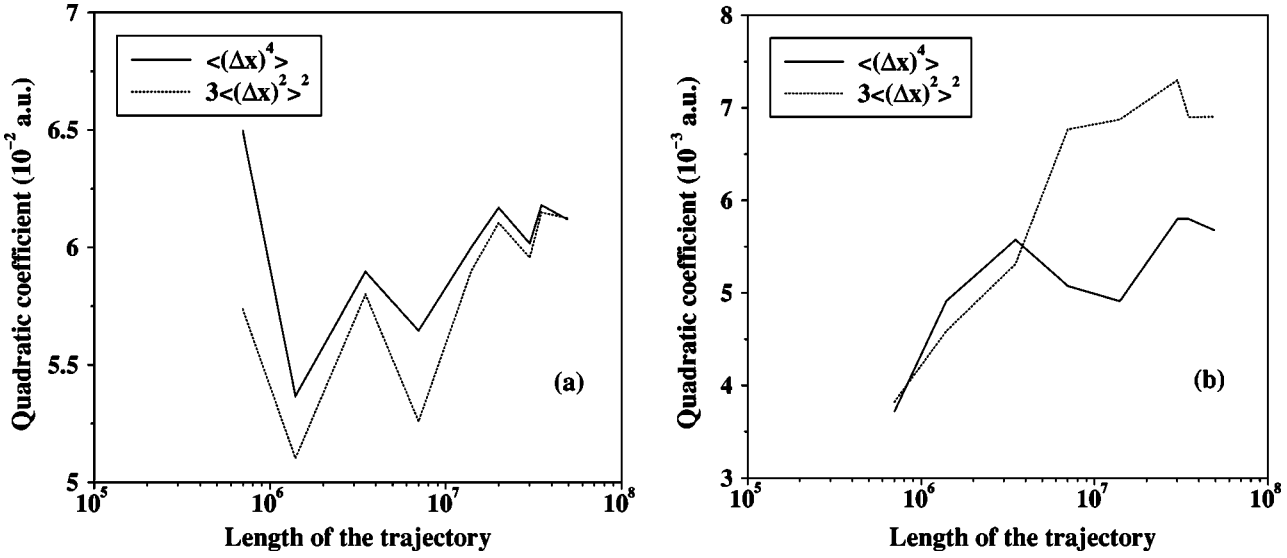

FIG. 11. Graphical representation of data contained in Table II (a) and Table III (b).

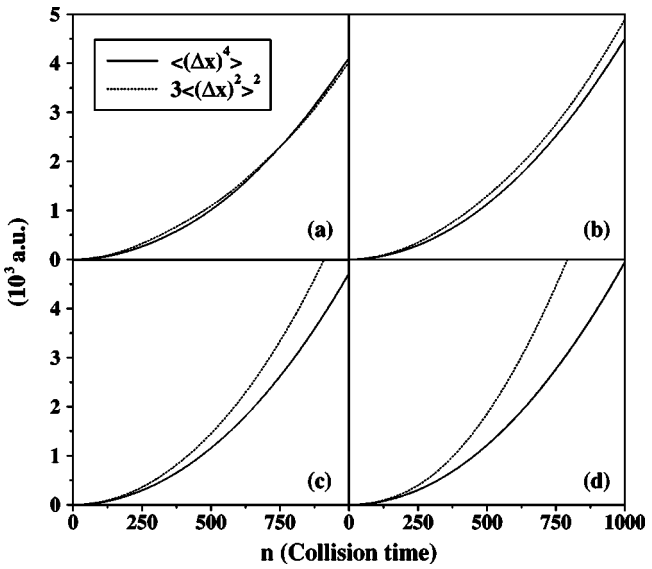

FIG. 13. The same as Fig. 12 for the polygonal billiard. (a) is for a time series up to 7×10^5, (b) 3.5×10^6, (c) 3×10^7, and (d) 4.9×10^7 collisions. Figures 12 and 13 show how the super Burnett coefficient is well defined for the Lorentz channel but not for the polygonal chain.

$$\lim_{t\to\infty}\int_\Gamma d\mu(x) f(\Phi^t x) g(x) = \int_\Gamma d\mu(x) f(x) \int_\Gamma d\mu(x) g(x). \tag{18}$$

The mixing condition implies a weaker property, *weak mixing* that requires the correlation functions to decay in the mean

$$\lim_{t\to\infty}\frac{1}{t}\int_0^t d\tau\left[\int_\Gamma d\mu(x) f(\Phi^\tau x) g(x) - \int_\Gamma d\mu(x) f(x) \int_\Gamma d\mu(x) g(x)\right]^2 = 0. \tag{19}$$

Another important property implied from mixing or weak mixing is *ergodicity* which establishes the equivalence between the phase space and the time averages,

$$\int_\Gamma d\mu(x) f(x) = \lim_{t\to\infty}\frac{1}{t}\int_0^t f(\Phi^\tau x) d\tau. \tag{20}$$

At this point we can introduce the phase space correlation function of two observables f and g

$$C_{fg}^\Gamma(t) = \int_\Gamma d\mu(x) f(\Phi^t x) g(x), \tag{21}$$

and the time correlation function as

$$C_{fg}^T(t) = \lim_{T\to\infty}\frac{1}{T}\int_0^T d\tau f(\Phi^{t+\tau} x) g(\Phi^\tau x). \tag{22}$$

In terms of these correlation functions ergodicity means

$$C_{f1}^\Gamma(t) = C_{f1}^T(t). \tag{23}$$

To study how statistical ensembles evolve we consider correlation functions such as

$$C_{fg}^\Gamma = \int_\Gamma d\mu(x) f(\Phi^t x) g(x) - \int_\Gamma d\mu(x) f(x) \int_\Gamma d\mu(x) g(x). \tag{24}$$

If they decay to zero for any choice of f and g then we have a system with the mixing property. It is relevant for our purposes to consider the Fourier transform of the correlation function, i.e., the *spectral function*:

$$S_{fg}(\omega) = \int_{-\infty}^{\infty} dt\, e^{i\omega t} C_{fg}^\Gamma(t). \tag{25}$$

The spectral function contains information on how the system evolves in time and which frequencies ω are important in such evolution. The frequencies can be real or complex. The role of this frequency spectrum, in short the *spectrum*, is better discussed in the context of spectral theories. Spectral theories for real frequencies were developed by Koopman [27] and Neunmann [28], in their context the spectrum may have a discrete and a continuous component. A singular continuous spectrum may also be possible [21]. In addition there is a spectral theory for complex frequencies that was developed by Pollicott [29] and Ruelle [30]. The complex frequencies are useful to deal with systems that show decay, either exponential or algebraic, that can be characterized in terms of the so-called Pollicot-Ruelle resonances. They are also useful in the description of decay properties in chaotic scattering [10,31]. In this article we only consider the real spectrum.

The spectral analysis of a system starts from the *evolution operator* $\hat{U}^t$ acting on the Hilbert space $\mathcal{H}=\mathcal{L}^2(\Gamma,\mu)$ of square integrable functions, with the scalar product $\langle f|g\rangle = \int_\Gamma f^*(x) g(x) d\mu(x)$. The evolution operator is defined through the action of the flow Φ^t as $\hat{U}^t f(x) = f(\Phi^t x)$. $\hat{U}^t$ is unitary if Φ^t is invertible and therefore its spectrum is on the unit circle. The properties of the flow can be described in terms of the spectral properties of $\hat{U}^t$. The application of the spectral theorem gives a spectral decomposition of $\hat{U}^t$ in all its components [32–34].

In general we have a spectral resolution of $\hat{U}^t$ with the form

$$\hat{U}^t = \int d\hat{E}_\omega\, e^{-i\omega t}, \tag{26}$$

where $\hat{E}_\omega$ is the spectral projector operator corresponding to the real eigenvalue ω. The decomposition is complete in the sense that $\int d\hat{E}_\omega$ is a resolution of the identity.

The nature of the spectrum can be analyzed if we have a realization of a spectral measure associated with a particular observable. For any function f within $\mathcal{L}^2(\Gamma,\mu)$, in the orthocomplement of the invariant subspace of unit eigenvalue,

$\mathcal{H}_c = \mathcal{H} \ominus \mathcal{H}_{(\omega=0)}$ with $\hat{E}_{(\omega=0)}\mathcal{H} = \mathcal{H}_0$, a spectral measure can be constructed as $\mu_f(\omega) = \langle f|\hat{E}_\omega f\rangle$.

The spectral measure is related to the autocorrelation function of f in the following manner

$$C_{ff}^{\Gamma}(t) = \langle f|\hat{U}^t f\rangle = \int \langle f|d\hat{E}_\omega f\rangle e^{-i\omega t} = \int d\mu_f(\omega) e^{-i\omega t}, \tag{27}$$

where we have used Eq. (26) and $d\mu_f(\omega) = \langle f|\hat{E}_{\omega+d\omega} f\rangle - \langle f|\hat{E}_\omega f\rangle$. In this manner the spectral measure associated with f is the inverse Fourier transform of the autocorrelation function of f. The nature of the spectrum is contained in $d\mu_f(\omega)$ or its cumulative function

$$\int_{\omega_{min}}^{\omega} d\mu_f(\omega') = F_f(\omega). \tag{28}$$

If there is a point spectrum then $F_f(\omega)$ will be a staircase function. If on the other hand the spectrum is continuous the cumulative function will be a continuous function and $dF_f(\omega)/d\omega > 0$. A singular continuous spectrum will give rise to a *devil staircase*–type curve for $F_f(\omega)$.

If for any choice of $f \in \mathcal{H}$ the spectrum is continuous then the system is mixing. However, if there is a point spectrum contribution the system cannot be mixing or even weak mixing. The presence of the weak-mixing property without mixing has been studied and related to the existence of singular continuous components in the spectrum [21].

As it has been mentioned before, a system with continuous spectrum, and for which the autocorrelation function of some observable f decays fast enough, may exhibit Gaussian fluctuations such that [10,32]

$$\lim_{T\to\infty} \mu\left\{ x, \frac{\int_0^T f(\Phi^t x)dt - T\langle f\rangle_\mu}{\sqrt{2D_f T}} < y \right\} = \frac{1}{\sqrt{2\pi}} \int_{-\infty}^{y} e^{-z^2/2} dz, \tag{29}$$

where D_f is a generalized diffusion coefficient defined by the variance

$$D_f = \lim_{T\to\infty} \frac{1}{2T} \left\langle \left[\int_0^T f(\Phi^t x)dt - T\langle f\rangle_\mu \right]^2 \right\rangle_\mu . \tag{30}$$

The generalized diffusion coefficient is related to the autocorrelation function of f by the Green-Kubo formula

$$D_f = \frac{1}{2} \int_{-\infty}^{\infty} d\tau\, C_{ff}^{\Gamma}(\tau) \tag{31}$$

with the condition $\lim_{T\to\infty}(1/T)\int_{-T}^{T} d\tau |\tau| C_{ff}^{\Gamma}(\tau) = 0$. In terms of the spectral function $S_{ff}(\omega)$ it follows then

$$2D_f = S_{ff}(0). \tag{32}$$

This equation links the behavior of the short frequency modes with transport, encoded by the generalized diffusion constant D_f at dynamical level. In the case of $f = v$ we recover Eq. (17). To summarize, the spectral and correlation functions are just different representations of the same object. Furthermore, they contain information about invariant properties such as mixing, weak mixing, or ergodicity. In particular, for systems with continuous spectrum and fast enough decay of correlations, generalized transport coefficients may be defined and the Einstein relation and the Green-Kubo formula are equivalent. In addition, the behavior of the spectral measure at zero frequency fixes the generalized diffusion coefficient.

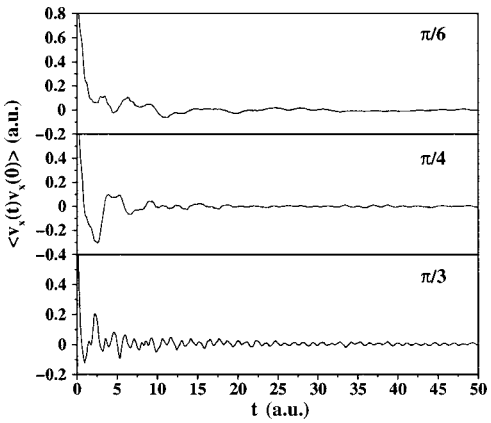

FIG. 14. Velocity autocorrelation functions for $\phi_2 = \pi/6$, $\pi/4$, and $\pi/3$.

A. Numerical results

As we have already emphasized, the velocity autocorrelation function (VACF) plays an important role in the analysis of diffusion because of the Green-Kubo formula (17). If the VACF decays in a convenient manner then there exists a well defined diffusion coefficient.

We have numerically obtained the VACF in the cases of $\phi_2 = \pi/3$, $\pi/4$ and $\pi/6$ for 10^6 particles, initially distributed at random in one fundamental cell, and integrated their trajectories over 2^{15} time steps with $\Delta t = 10^{-2}$. The results are shown in Fig. 14. The first point to notice is the oscillatory form in the decay of the VACF, in contrast with the monotonous decay in the Lorentz gas. In any case, the decay of the VACF can be considered as an indication that the systems treated are mixing. Nonetheless, mixing implies that correlation functions decay for *all* observables and not just for the velocity. From Eq. (17) we can obtain the diffusion coefficient by integrating the VACF. In doing so we see that the Green-Kubo formula gives results in good agreement with those obtained from the Einstein relation for diffusion. In the system $\pi/3$ the correlation function does not seem to decay fast enough, and hence the diffusion coefficient diverges. See Fig. 15.

B. Spectral analysis

It is also possible to extract information about the spectrum from the VACF as previously discussed. If we use Eqs. (25) and (27) we can obtain the spectral function. In Fig. 16 is plotted the spectral functions for the correlation functions

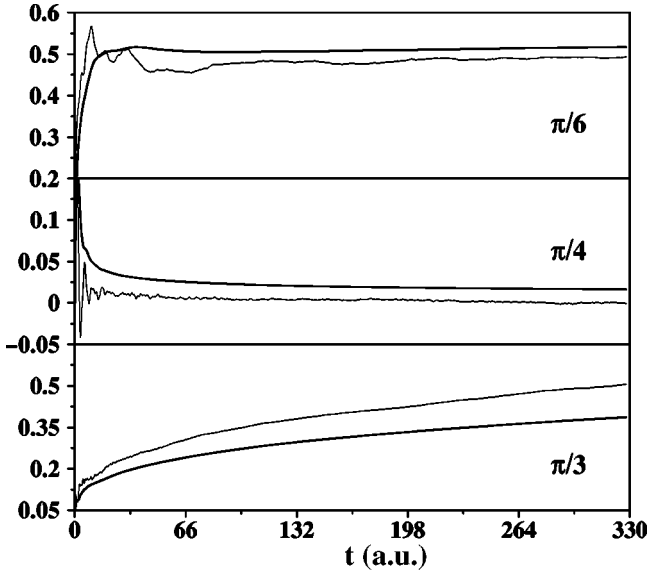

FIG. 15. The cumulative integral of the velocity autocorrelation function (thin line) and $\langle (x(t)-x(0))^2\rangle/2t$ (thick line).

numerically obtained, which are in good agreement with the expectations of Eq. (32) for those cases in which correlations decay.

The measure so reconstructed may exhibit interesting scaling properties [13,21], in particular the correlation and information dimensions. The multifractal analysis of the measure can be done as follows. The spectral interval is divided in subintervals $I_{N,\alpha}$ ($\alpha=1,\ldots,2^N$). The generalized dimensions of the measure $d\mu_f(\omega)$, $D_1(\mu_f)$, and $D_2(\mu_f)$, are the scaling exponents defined by

$$\chi_{1,N}=\sum_{\alpha=1}^{2^N}\mu_f(I_{N,\alpha})\ln\mu_f(I_{N,\alpha})\sim -ND_1\ln 2, \qquad (33)$$

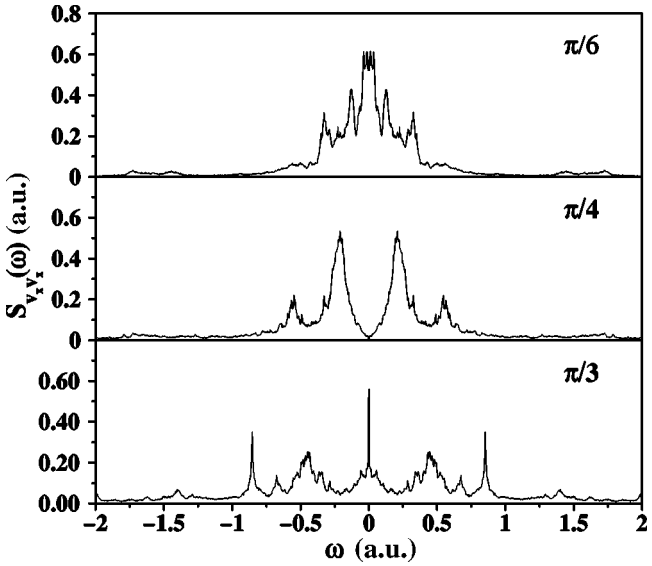

FIG. 16. Spectral functions corresponding to the velocity autocorrelation functions in Fig. 14.

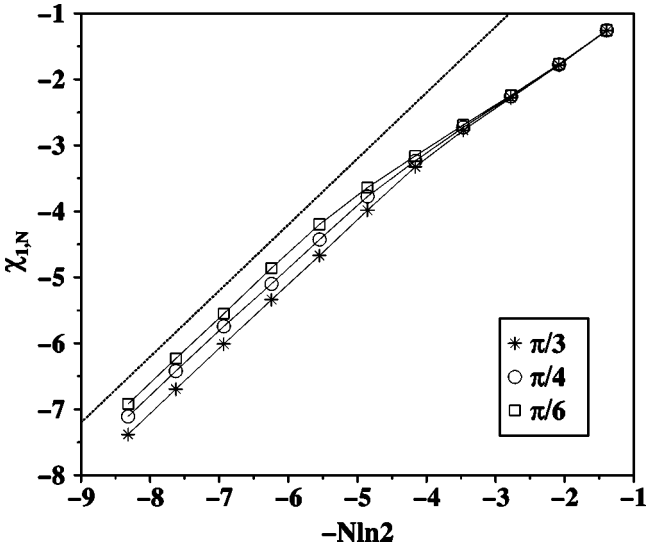

FIG. 17. D_1 coefficient (see text) for the spectrum derived from the velocity autocorrelation function. The dotted line corresponds to a line with slope -1.

$$\chi_{2,N}=\ln\sum_{\alpha=1}^{2^N}\mu_f^2(I_{N,\alpha})\sim -ND_2\ln 2. \qquad (34)$$

It is known [21] that under certain assumptions D_1 coincides with the Hausdorff dimension of the measure. The D_2 coefficient is related to the integrated correlation function. In the case of continuous spectrum the integrated correlation

$$C_f^{int}(t)=\frac{1}{t}\int_0^t d\tau|C_f(\tau)|^2 \qquad (35)$$

of an observable f is expected to decay to zero as

$$C_f^{int}(t)\sim t^{-D_2} \qquad (36)$$

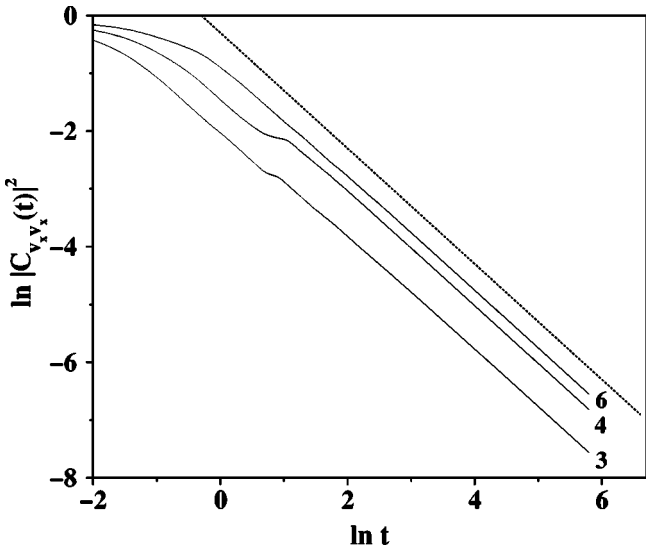

FIG. 18. Integrated velocity autocorrelation functions; see Eq. (35). The dotted line corresponds to a line with slope -1.

FIG. 19. Schematic representation of a polygonal billiard chain put in contact with two heat reservoirs of temperature T_0 and T_1.

with D_2 defined in Eq. (34). The multifractal analysis of the spectral measure we obtained (see Fig. 17) indicates that D_1 is in all cases almost one, while our data is not precise enough to give a good estimation of D_2. In any case, the integrated correlation functions, see Fig. 18 and Eq. (36), decay as t^{-1}; this suggests again that the systems could be mixing. A more precise statement about D_2 requires us to have the VACF for longer time. This implies integrating a much larger ensemble of particles (to improve the statistics) further in time.

V. HEAT CONDUCTIVITY

We also studied the heat conductivity of the polygonal chain. There is a major interest in simple models that may exhibit heat conductivity. A series of studies (in which no Markovian limit is involved) has been devoted to one-dimensional chains of nonlinear coupled oscillators and there is strong numerical evidence [37] (see [35,36] for recent developments) for the validity of the Fourier heat conduction law in the so-called *ding-a-ling* (where oscillators exchange energy via intermediate hard spheres), while the situation is considerably more complicated in the Fermi-Pasta-Ulam chain (where oscillators are coupled by third and fourth order nonlinear terms) where, even above the chaoticity threshold, heat conductivity seems abnormal [39]. Both systems exhibit exponential instability in numerical simulations, thus positivity of Lyapunov exponents cannot presumably be a sufficient condition for inducing normal transport properties. More recently anomalous heat transport has been reported for a diatomic one-dimensional ideal gas [38].

In the case of the Lorentz channel [16] normal heat conductivity is observed. We will study in which cases (ϕ_2 values) the heat conduction is normal in our polygonal billiards. More recent results [12] suggest that it is possible to have normal heat conduction in this type of system. To induce heat transport we have put two heat reservoirs at the left- and right-hand sides of the billiard chain (see Fig. 19). The heat reservoirs are modeled by stochastic kernels of Gaussian type,

$$P(v)=\pm\frac{|v|}{T}e^{-v^2/2T}, \tag{37}$$

where v is the x component of the velocity in the collision with the heat bath at temperature T. The minus sign is taken at the right-hand side and the plus sign at the left reservoir. The Boltzmann's constant is set to one. A comment is in order here; in our simulations, when the particle collides with the heat reservoir, the y component of the velocity is conserved and the x component is changed in agreement with

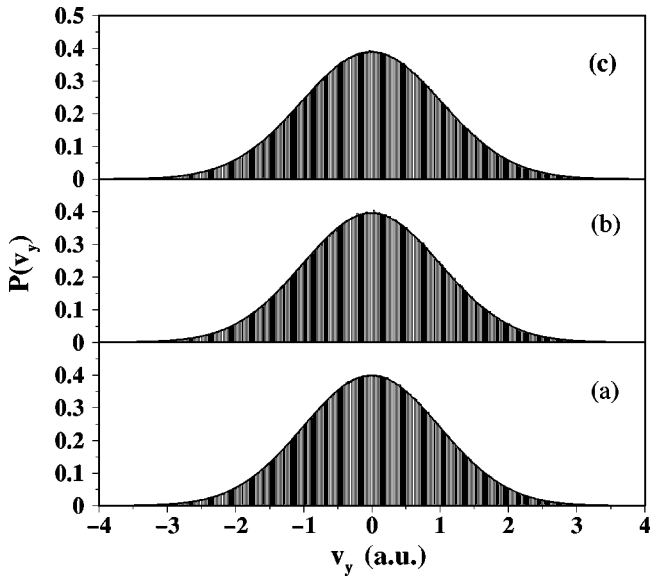

FIG. 20. Normalized velocity distribution (v_y component). In (a) the distribution at the left heat reservoir ($T_0=1.00$). In (b) the distribution at the center of the billiard chain and in (c) the distribution at the right reservoir ($T_1=1.05$). The thick lines are the best Gaussian fitting of the histograms.

the distribution (37). One may wonder if it is also necessary to distribute the v_y velocity component according to a Maxwellian distribution. In fact this is not needed in our case. Actually, what happens is that after many collisions, in spite of the fact that only v_x is randomized, the v_y is finally distributed according to a distribution that numerically seems very close to a Maxwell distribution. To illustrate this point we have computed the v_y velocity at each collision with a heat reservoir (we remember that we keep this component of the velocity unchanged during the collision with the heat baths) and evaluated its distribution. In Fig. 20 we show the results of a typical simulation for heat reservoirs with temperatures $T_0=1(a)$ and $T_1=1.05(c)$. It is clear that the v_y distribution is Maxwellian with the correct temperature, although this component of the velocity is not taken at random during the collisions with the heat reservoir, as is the case for v_x.

Following Alonso *et al.* [16] we computed the temperature field at the stationary state. To achieve this task we defined a grid of points in configuration space (x_i,y_j), $(i=1,\ldots,N_x, j=1,\ldots,N_y)$ around which there is a cell C_{ij}. This set of cells defines a partition of the configuration space. During the time evolution the particle crosses the cell C_{ij} in N_{ij} occasions; let us call t_α and $E_\alpha(ij)$ the time spent by the particle and its energy during the α visit to the cell ($\alpha=1,\ldots,N_{ij}$). We define a coarse grained temperature field $T(ij)$ as the average

$$T(ij)=\langle E\rangle_{ij}=\frac{\sum_{\alpha=1}^{N_{ij}} t_\alpha E_\alpha(ij)}{\sum_{\alpha=1}^{N_{ij}} t_\alpha}. \tag{38}$$

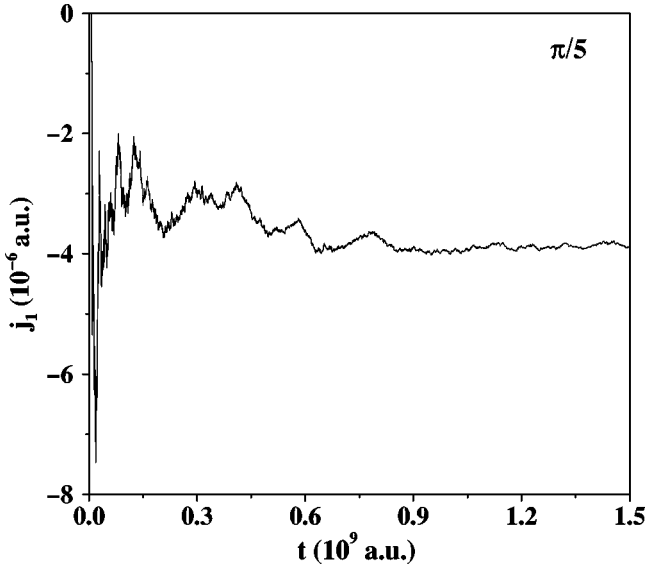

FIG. 21. Typical behavior (for $\phi_2=\pi/5$) of the heat current at the boundaries as a function of time. After many collisions the stationary state is reached and the current stabilizes at a constant value.

This procedure defines a two-dimensional field. As we have mentioned, the transport takes place along the x direction so we will focus on the $x-T(x,y)$ plane at some stages.

Another quantity of interest is the heat flux at the stationary state. The kinetic energy is constant within the billiard and only changes when there is a collision with a reservoir, in which case it suffers a change in energy

$$\Delta E_k = E_{in} - E_{out}, \tag{39}$$

with k an index for the collision. If we sum over N of such events that take place over a time t_N we have for the heat flux

$$j_n = \frac{1}{t_N} \sum_{k=1}^{N} \Delta E_k . \tag{40}$$

The stationary state is reached if for long enough time t_N the heat flux is constant. In Fig. 21 we show a typical heat current obtained during the simulations. It is clear how the heat current stabilizes at a constant value once the system reaches the stationary state. We have numerically computed the temperature field, as defined in Eq. (38), as well as the heat current as a function of the system size. We have analyzed how the heat flux scales with the system size. For a single particle simulation and for a system with n fundamental cells (not to be confused with the cells defined for the evaluation of the temperature) we have a flux $j_1(n)$. In order to implement the thermodynamic limit correctly we should study the current $j_n(n)=nj_1(n)$ (for a density of one particle per fundamental cell). In our numerical simulations we found that $j_n(n)$ scales as $\gamma n^{-\delta}$. We have to distinguish the cases $\phi_2=\pi/3$ and $\phi_2=\pi/4$ from $\phi_2=\pi/q$ $(q=5,6,7,8,9)$.

For $\phi_2=\pi/3$ is clear that the heat flux is such that it leads to an infinite heat conductivity coefficient. In this case $\delta=0.72$. For $\phi_2=\pi/4$ the heat current scales with $\delta=1.63$, which yields a zero heat conductivity coefficient. All the other systems have scaling exponents very close to one (see Fig. 22).

The temperature fields (see Fig. 23) are linear for small temperature differences and show some structure induced by the geometry of the boundaries. We can conclude then that for $\phi_2=\pi/q$ $(q=5,6,7,8,9)$ the heat conduction is normal, but not for the cases $\phi_2=\pi/3$ and $\pi/4$, which are superdiffusive and subdiffusive, respectively.

As noticed in [16] the temperature fields scale with length as $T_{[0,L]}(x)=T_{[0,1]}(x/L)$. In Fig. 24 we show the typical density plots of the two-dimensional temperature field. In all the systems we have a complete consistency with the results of the diffusive properties of the billiard chain.

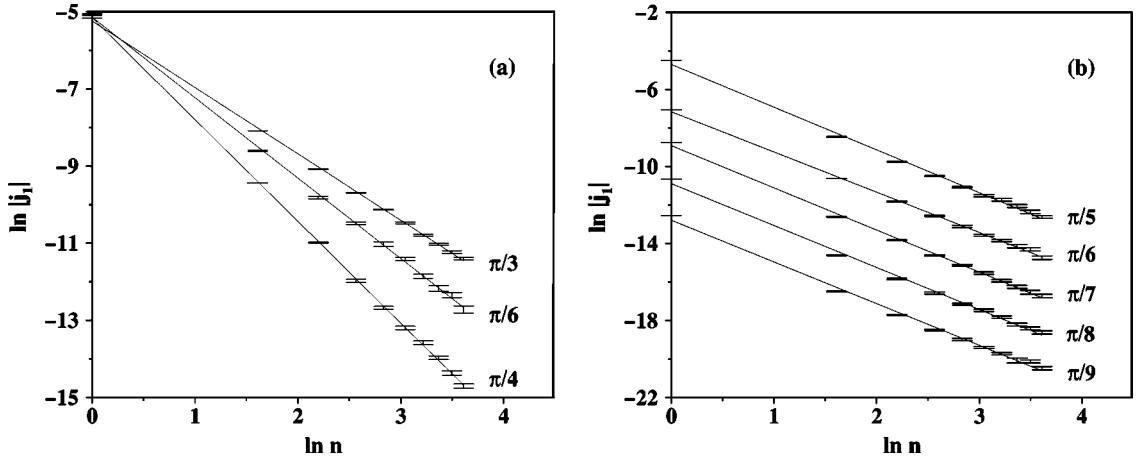

FIG. 22. Scaling behavior of the heat flux for the systems $\phi_2=\pi/3,\pi/4$ and $\pi/6$ (a), and $\phi_2=\pi/q$ $(q=5,6,7,8,9)$ (b). The figures show how the systems $\phi_2=\pi/3$ and $\pi/4$ have infinite and zero heat conductivity constant, respectively. The other cases show a scaling behavior compatible with a well defined heat conductivity coefficient in the thermodynamic limit. In (b) the curves have been translated along the y axis in order to compare them.

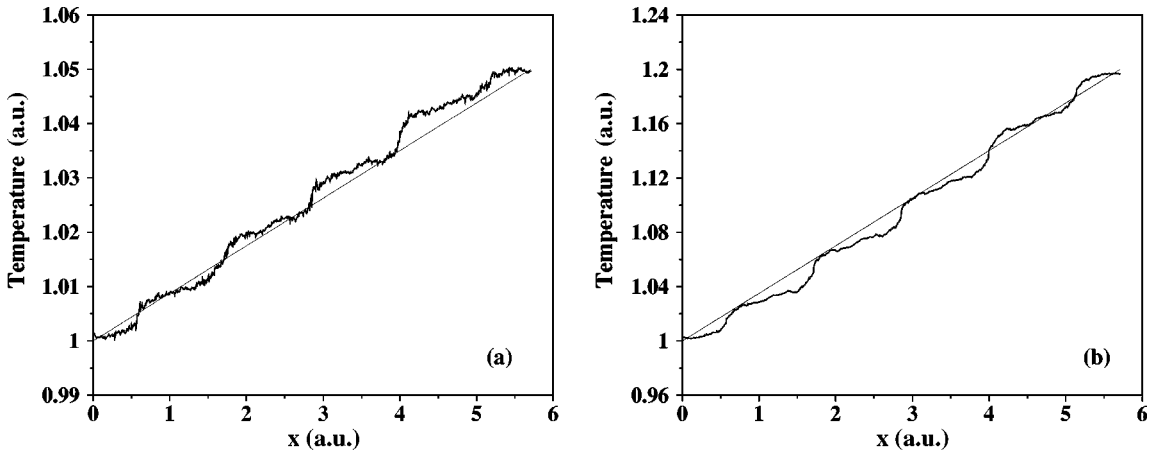

FIG. 23. Temperature profiles in the $x-T(x,y)$ plane for a system with $\phi_2=\pi/6$, five fundamental cells and $T_0=1, T_1=1.05$ (a) and $T_0=1, T_1=1.2$ (b). The straight lines are the ideal Fourier profiles.

VI. CONCLUDING REMARKS

In conclusion, while one can agree that most of the aspects in relation to the links between chaotic dynamics and transport are more or less well known, much remains to be done for nonchaotic systems with some degree of stochasticity, which has in this case a very different origin to the one in chaotic systems. In this regard, polygonal billiards are simple prototype systems that constitute a natural step forward in the study of the connections between transport and dynamical properties. It is only recently that there is convincing numerical evidence [9,11] suggesting that some classes of polygonal billiards may have well defined transport properties. Our goal in this work has been to go deeply in these matters, extending our previous research on the Lorentz channel [16] to polygonal chains.

In our study of a family of polygonal chains we have analyzed the diffusion of ensemble of particles as well as the heat conduction. Our strategy has been twofold. On one hand, we computed the mean square displacement and verified that for some members of the family it behaves diffusively, while for others the mean square displacement behaves in a strange way (either subdiffusively or superdiffusively). On the other hand, the validity of the diffusion equation has been explored through the study of the dispersion relation for diffusion for long wavelengths [see Eqs. (5) and (10)].

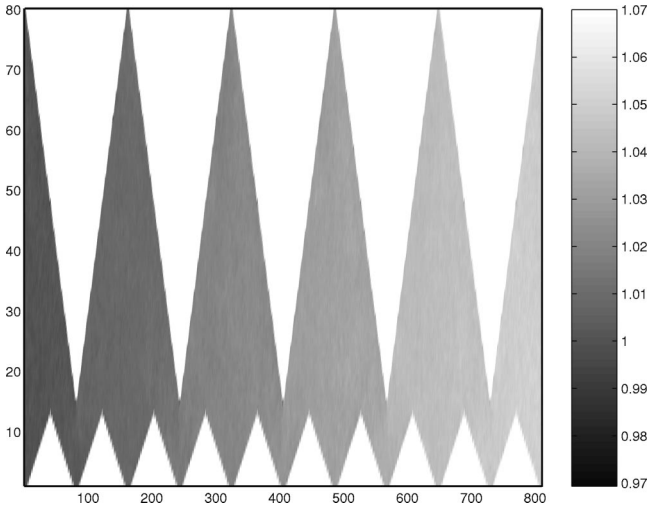

FIG. 24. Density plot of the temperature field for $\phi_2=\pi/6$, five fundamental cells, $T_0=1$, and $T_1=1.05$.

In both cases our main conclusion is that there are some members of the family of systems studied that satisfy the Einstein relation for diffusion. For these systems we also showed that the dispersion relation for hydrodynamic modes is compatible with the diffusion equation.

Single particle simulations give us the same results. An important point is that any member of the family has a well defined super Burnett coefficient.

The analysis of the velocity autocorrelation functions and their spectral functions lead us to the same conclusions. For those systems that present a diffusive or subdiffusive behavior, the Green-Kubo formula holds and gives us the correct diffusion coefficient (zero in the case of subdiffusion). The spectral function analysis is in agreement with these results. The velocity autocorrelation functions oscillate and decay, so such decay has to be analyzed more carefully, taking into account the oscillations.

The multifractal analysis of the spectral measure reveals that the Hausdorff dimension of the spectrum is probably one for all systems. Our simulations do not allow us to give a precise value of the correlation dimension D_2. Nonetheless there is numerical evidence that supports the statement that the integrated correlation function decays as $\sim t^{-D_2}$. Our integrated autocorrelation functions decay as $\sim t^{-1}$. All this data gives us indications that the polygonal billiards studied may be mixing.

Finally, we have studied heat transport in the polygonal chain and found that, naturally, those systems which present diffusion also have normal heat transport. On the contrary, for the systems with subdiffusion ($\phi_2=\pi/4$) the computations lead to a zero heat conductivity coefficient, and to an infinite heat conductivity coefficient for the superdiffusive system ($\phi_2=\pi/3$).

With respect to the nature of the nonequilibrium station-

ary states for diffusion and heat conduction it would be interesting to study if fractal or self-similar structures emerge, as those observed for the Lorentz gas and other models [10].

As a last point let us mention that our results come from finite time numerical simulations; it would be of great interest to have some mathematical results of these delicate matters.

ACKNOWLEDGMENTS

D.A. thanks R. Artuso, G. Casati, P. Gaspard, I. Guarneri, and G. Nicolis for fruitful discussions at different stages of this work at Como and Brussels. D.A. also thanks Professor H. Van Beijeren for his many suggestions and his careful reading of the manuscript and L. Rondoni for his discussions about Fourier law. Support has been provided by Gobierno de Canarias (PI2000/111), Ministerio de Ciencia y Tecnología (BFM2001-3349 y BFM2001-3343). I.d.V. is financially supported by the Ministerio de Ciencia y Tecnología.

APPENDIX: DEFINITION OF THE TEMPERATURE FIELD

The point particle is located at $r_t=(x,y)$ at time t; the number density $n(z,t)$ is defined as

$$n(z,t)=\frac{1}{t}\int_0^t d\tau\,\delta^{(2)}(z-r_\tau), \tag{A1}$$

where $\delta^{(2)}(r)$ is Dirac's delta. If we adopt an *approximate* representation of $\delta^{(2)}(r)$ as

$$\frac{1}{\epsilon^2}\chi_\epsilon(z-r_t), \tag{A2}$$

with $\chi_\epsilon(z-r_t)$ the characteristic function of a cell centered at z with surface ϵ^2 such that is one if r_t is within the cell and zero otherwise. Notice that for $\epsilon\to 0$ we recover Dirac's delta from Eq. (A2). For this *finite* resolution the *coarse-grained* number density is

$$n_\epsilon(z,t)=\frac{1}{t\epsilon^2}\int_0^t d\tau\,\chi_\epsilon(z-r_\tau). \tag{A3}$$

In the same manner we define the mean kinetic energy as

$$E(z,t)=\frac{1}{t}\int_0^t d\tau\,E(r_\tau)\,\delta^{(2)}(z-r_\tau), \tag{A4}$$

and its coarse-grained approximation

$$E_\epsilon(z,t)=\frac{1}{t\epsilon^2}\int_0^t d\tau\,E(r_\tau)\chi_\epsilon(z-r_\tau). \tag{A5}$$

The coarse-grained temperature field is defined from the assumption of local equilibrium and is

$$T_\epsilon(z,t)=\frac{\int_0^t d\tau\,E(r_\tau)\chi_\epsilon(z-r_\tau)}{\int_0^t d\tau\,\chi_\epsilon(z-r_\tau)}. \tag{A6}$$

If during the time interval $(0,t)$ the trajectory r_τ visits the cell centered at z N times, and in each visit spends a time t_α, then it follows from Eq. (A6) that

$$T_\epsilon(z,t)=\frac{\sum_{\alpha=1}^{N} t_\alpha E(z,t_\alpha)}{\sum_{\alpha=1}^{N} t_\alpha}. \tag{A7}$$

If the time t is long enough we can reach a stationary state and $T_\epsilon(z,t)$ can be considered an approximation of the stationary temperature field of the system at scale ϵ. If the two-dimensional coordinate z is indexed by ij we recover the expressions used throughout the paper.

[1] L.A. Bunimovich, Commun. Math. Phys. **65**, 295 (1979); L.A. Bunimovich and Ya.G. Sinai, *ibid.* **78**, 247 (1980); **78**, 479 (1981); L.A. Bunimovich, Physica D **33**, 58 (1988).
[2] A. Knauf, Commun. Math. Phys. **109**, 1 (1987).
[3] L.A. Bunimovich and H. Spohn, Commun. Math. Phys. **176**, 661 (1996).
[4] P. Gaspard, J. Stat. Phys. **68**, 673 (1992).
[5] S. Tasaki and P. Gaspard, J. Stat. Phys. **81**, 935 (1995).
[6] R. Artuso, Phys. Lett. A **160**, 528 (1991).
[7] J.R. Dorfman and P. Gaspard, Phys. Rev. E **51**, 28 (1995).
[8] G. Gallavotti and E.G.D. Cohen, Phys. Rev. Lett. **74**, 2694 (1995); J. Stat. Phys. **80**, 931 (1995); G. Gallavotti, *ibid.* **84**, 899 (1996); Phys. Rev. Lett. **77**, 4334 (1996).
[9] S. Lepri, L. Rondoni, and G. Benettin, J. Stat. Phys. **99**, 857 (2000); G. Benettin and L. Rondoni, Math. Phys. Electron. J. **7**, 22 (2001).
[10] P. Gaspard, *Chaos, Scattering and Statistical Mechanics* (Cambridge University Press, Cambridge, England, 1998).
[11] C.P. Dettmann, E.G.D. Cohen, and H. Van Beijeren, Nature (London) **401**, 875 (1999); C.P. Dettmann and E.G.D. Cohen, J. Stat. Phys. **101**, 775 (2000).
[12] B. Li, L. Wang, and B. Hu, Phys. Rev. Lett. **88**, 223901 (2002); B. Li, J. Wang, and G. Cassati, e-print cond-mat/0208098.
[13] R. Artuso, Physica D **109**, 1 (1997).
[14] G. Casati and T. Prosen, Phys. Rev. Lett. **83**, 4729 (1999).
[15] J.L. Lebowitz and H. Spohn, J. Stat. Phys. **19**, 633 (1978).
[16] D. Alonso, R. Artuso, G. Casati, and I. Guarneri, Phys. Rev. Lett. **82**, 1859 (1999).
[17] P. Gaspard and J.R. Dorfman, Phys. Rev. E **52**, 3525 (1995).
[18] L. Van Hove, Phys. Rev. **95**, 249 (1954).
[19] P.J. Richens and M.V. Berry, Physica D **2**, 495 (1981).
[20] E. Gutkin, Physica D **19**, 311 (1986).

[21] R. Artuso, I. Guarneri, and L. Rebuzzini, Chaos **10**, 189 (2000).
[22] E. Gutkin, Max-Planck-Institute für Mathematik in der Naturwissnschaften, Leipzig Report No. 103, 2001.
[23] Ya. Vorobets, Sb. Math. **188**, 389 (1997).
[24] R. Balescu, *Statistical Dynamics* (Imperial College Press, London, 1997).
[25] H. Van Beijeren, Rev. Mod. Phys. **54**, 195 (1982).
[26] P. Gaspard and I. Claus, Philos. Trans. R. Soc. London, Ser. A **360**, 303 (2002); P. Gaspard, I. Claus, T. Gilbert, and J.R. Dorfman, Phys. Rev. Lett. **86**, 1506 (2001).
[27] B.O. Koopman, Proc. Natl. Acad. Sci. U.S.A. **17**, 17 (1931).
[28] J. von Neumann, Proc. Natl. Acad. Sci. U.S.A. **18**, 70 (1932).
[29] M. Pollicot, Invent. Math. **81**, 413 (1986); **85**, 147 (1986).
[30] D. Ruelle, Phys. Rev. Lett. **56**, 405 (1986).
[31] P. Gaspard and D. Alonso Ramírez, Phys. Rev. A **45**, 8383 (1992).
[32] *Dynamical Systems II*, edited by Ya. G. Sinai, Encyclopaedia of Mathematical Sciences Vol. 2 (Springer-Verlag, Berlin, 1985).
[33] V.I. Arnold and A. Avez, *Ergodic Problems of Classical Mechanics* (Benjamin, New York, 1968).
[34] M. Reed and B. Simon, *Methods of Modern Mathematical Physics: I, Functional Analysis* (Academic, New York, 1980).
[35] T. Prosen and M. Robnik, J. Phys. A **25**, 3449 (1992).
[36] D.J.R. Mimnagh and L.E. Ballentine, Phys. Rev. E **56**, 5332 (1997).
[37] G. Casati, J. Ford, F. Vivaldi, and W.M. Visscher, Phys. Rev. Lett. **52**, 1861 (1984).
[38] G. Casati and T. Prosen, e-print cond-mat/0203331.
[39] S. Lepri, R. Livi, and A. Politi, Phys. Rev. Lett. **78**, 1896 (1997); A. Fillipov, Bambi Hu, Baowen Li, and A. Zeltser, J. Phys. A **31**, 7719 (1998); Bambi Hu, Baowen Li, and Hong Zhao, Phys. Rev. E **57**, 2992 (1998); H. Kaburaki and M. Machida, Phys. Rev. Lett. **181**, 85 (1993); A. Kato and D. Jou, Phys. Rev. E **64**, 052201 (2001).
[40] We follow the notation of [10].